Sulforaphane attenuates cisplatin-induced acute kidney injury by inhibiting oxidative stress, inflammation and apoptosis via regulation of NRF2

ZEYU WU[1*], MENGTING LU[2*], LEI XU[1], MING LUO[1], LIMEI SHAN[1], HONGXIA XING[2], WENWEN LI[2] and JUNLING QIAN[1]

[1]Department of Cardiothoracic Surgery, Nanjing Jiangning Hospital, Nanjing Medical University, Nanjing, Jiangsu 211100, P.R. China; [2]Department of Nephrology, Sir Run Run Hospital, Nanjing Medical University, Nanjing, Jiangsu 211112, P.R. China

Received October 21, 2025; Accepted April 24, 2026

DOI: 10.3892/mmr.2026.13944

Abstract. Cisplatin-induced acute kidney injury (CI-AKI) is one of the most common comorbidities in patients undergoing chemotherapy, notably limiting the clinical use of cisplatin. However, the pathogenesis of CI-AKI remains to be fully elucidated. Sulforaphane (SFN), a NRF2 agonist, exhibits anti-inflammatory, antioxidant and anti-apoptotic effects, thus SFN exerts protective effects in kidney injury diseases. However, the possible role and underlying mechanisms of SFN in CI-AKI remain ambiguous. An *in vivo* model of CI-AKI was constructed using C57BL/6 mice that were administered a single intraperitoneal cisplatin injection (20 mg/kg) and conditionally treated with SFN (10 mg/kg). Serum creatinine (Scr) and blood urea nitrogen (BUN) levels were detected by biochemical analysis. Western blotting was performed to assess the expression of renal injury markers, as well as the apoptosis-related proteins cleaved caspase-3, caspase-3, Bax and Bcl-2. Furthermore, hematoxylin and eosin and periodic acid-Schiff staining were employed to detect renal tissue lesions in mice, and TUNEL staining was used to evaluate the apoptosis of renal tissues in each group *in vivo*. Immunohistochemistry was used to assess the expression of inflammatory marker F4/80 in mouse renal tissues, and ELISA was used to detect the expressions of the inflammatory markers IL)-1β, IL-6 and tumor necrosis factor-α (TNF-α) in the serum of mice in each group. DCFH-DA) analysis was used to detect reactive oxygen species (ROS) levels and biochemical analysis was used to evaluate the expression levels of malondialdehyde, superoxide dismutase and glutathione. Finally, western blotting and immunohistochemistry were performed to evaluate the expression of NRF2. An *in vitro* model of CI-AKI was constructed using HK-2 cells induced by cisplatin (10 μg/ml) that were conditionally treated with one or both of SFN (5 μM) and the NRF2 inhibitor ML385 (1.9 μM). Reverse transcription-quantitative PCR was performed to evaluate the expression of NRF2. Cell Counting Kit-8 assay was performed to assess the viability of HK-2 cells in different groups, whereas flow cytometry was used to assess the apoptosis of HK-2 cells in different groups. DCFH-DA analysis was performed to evaluate the expression of ROS in different treatment groups. Furthermore, ELISA was used to evaluate the expressions of IL-1β, IL-6 and TNF-α in each group. SFN notably decreased the serum levels of Scr and BUN and decreased the expression levels of kidney injury molecule-1 and neutrophil gelatinase-associated lipocalin in the cisplatin-induced model group. Histopathological examination revealed attenuated renal structural damage and preserved tubular architecture in the SFN intervention group. Furthermore, SFN notably inhibited the apoptosis, inflammation and oxidative stress of renal tissues induced with cisplatin. Additionally, SFN markedly upregulated NRF2. *In vitro*, the NRF2 inhibitor ML385 partially attenuated the effects of SFN on the viability, apoptosis, inflammation and oxidative stress of HK-2 model cells. The present study indicated that SFN exerted its nephroprotective effect through NRF2-mediated anti-inflammatory, antioxidant and anti-apoptotic mechanisms, positioning SFN as a promising therapeutic candidate for clinical management of chemotherapy-associated kidney injury.

Correspondence to: Professor Junling Qian, Department of Cardiothoracic Surgery, Nanjing Jiangning Hospital, Nanjing Medical University, 169 Hushan Road, Nanjing, Jiangsu 211100, P.R. China
E-mail: warmyrtm@163.com

*Contributed equally

Key words: cisplatin-induced acute kidney injury, sulforaphane, oxidative stress, inflammation, apoptosis, nuclear factor erythroid-2-related factor 2

Introduction

Malignant tumors represent one of the leading causes of human mortality, and the primary methods for treating tumors are surgical resection and chemotherapy (1). Cisplatin, also known as cis-dichlorodiamine platinum, is one of the most prevalent and effective chemotherapy drugs at present. Cisplatin is predominantly used to treat breast, ovarian, esophageal, bladder, head and neck cancers, as well as non-small cell lung

cancer and other solid tumors (2-4). Mechanistically, cisplatin predominantly induces tumor cell death by cross-linking with purine bases in DNA, resulting in DNA damage that subsequently activates various apoptotic or necrotic pathways (5). However, cisplatin has been shown to not only kill tumor cells but also normal cells, resulting in toxic side effects, such as ototoxicity, neurotoxicity, bone marrow suppression and nephrotoxicity, which severely limit the clinical application of cisplatin (6). Nephrotoxicity represents the dose-limiting factor for cisplatin use and remains the predominant factor limiting its clinical application (7). A study has shown that 30-40% of patients treated with cisplatin experience nephrotoxicity, which predominantly manifests as acute kidney injury, depletion of salt or magnesium ions, and loss of urine-concentration function (8).

At present, drugs used clinically to alleviate or prevent cisplatin-induced acute kidney injury (CI-AKI) remain limited in their application due to various side effects (9). Additionally, the emergence of chimeric antigen receptor (CAR)-T-cell therapy has demonstrated notable potential for improving treatment of CI-AKI. A previous clinical trial has shown that although anti-CD19 CAR-T cells demonstrate notable clinical efficacy, their long-term safety and sustained therapeutic benefits represent ongoing translational challenges (10). Therefore, exploring adjuvant drugs that can effectively alleviate kidney injury during cisplatin chemotherapy will notably improve the clinical application of cisplatin.

The exact mechanisms of CI-AKI remain ambiguous. Several molecular mechanisms that contribute to CI-AKI pathogenesis include the uptake and accumulation of cisplatin, oxidative stress, the inflammatory response, cell apoptosis and necrosis (11,12). In particular, oxidative stress caused by the excessive generation of reactive oxygen species (ROS) is associated with CI-AKI pathogenesis (13). Cisplatin enters cells and generates ROS through normal metabolic processes, which deplete antioxidant substances, such as superoxide dismutase (SOD), glutathione (GSH) and malondialdehyde (MDA), and disrupt the dynamic balance of intracellular oxidation-reduction reactions, resulting in increased oxidative stress (14). In addition, the excessive production of ROS can activate the NF-κB) signaling pathway, upregulate the expression of pro-inflammatory factors, such as tumor necrosis factor-α (TNF-α) and interleukin (IL)-1β, and alter the activity of multiple signaling pathways that lead to cell apoptosis (15). Pro-inflammatory ILs have been shown to facilitate CI-AKI progression by recruiting neutrophils and inducing apoptosis of renal cells. However, anti-inflammatory ILs have been shown to attenuate CI-AKI by promoting regulatory T cell activity and suppressing pro-inflammatory cytokines (16).

Nuclear factor erythroid-2-related factor 2 (NRF2) is a common transcription factor that can regulate oxidative stress, drug detoxification and the inflammatory response through various pathways (17). Primarily, NRF2 can inhibit oxidative stress and activation of the NF-κB signaling pathway by suppressing the accumulation of intracellular ROS. Additionally, NRF2 has been shown to inhibit the proteasomal-degradation of IκB-α, a negative regulator of NF-κB, thereby suppressing the nuclear translocation of NF-κB (18). Therefore, activation of the NRF2 signaling pathway may confer protection against cisplatin-induced oxidative stress and inflammatory responses, thus mitigating subsequent tissue damage.

In a study on NRF2 activators, such as sulforaphane (SFN) and dimethyl fumarate in CI-AKI, SFN was found to significantly improve mitochondrial function in renal tubular cells, upregulate cortical NRF2 expression and downregulate the protein expression of its repressor Keap1, thereby alleviating oxidative stress and tubular damage induced by cisplatin (19). Dimethyl fumarate activated the NRF2 pathway to increase the expression of downstream cytoprotective gene NQO1, suppressed the production of inflammatory cytokines including TNF-α and IL-6, and effectively reduced cisplatin-induced renal tubulointerstitial fibrosis and tubular necrosis (19). SFN is the hydrolysis product of thiogluconate, which can be extracted from a number of vegetables, such as broccoli (20). Notably, SFN has been proven to be non-toxic, reliable, easy to obtain and inexpensive and exhibiting a broad range of application prospects (21). In addition, SFN has been shown to display a number of therapeutic effects, namely anti-inflammatory, antioxidant, anticancer effects, in animals (22). A previous study demonstrated that metabolites of SFN can be detected in all organs at up to 6 h after administration, with higher concentrations observed in the small intestine, prostate, lungs and kidneys, indicating that SFN is bioabsorbable (23). Furthermore, another study showed that AKI induced by medication or ischemia can be alleviated by SFN-activated NRF2 (24). Previous research found that SFN treatment in mouse models of diabetic nephropathy markedly reduced renal damage, which may be due to the protective effect of SFN-mediated NRF2 pathway activation on renal tissue (25).

However, it remains to be fully elucidated whether SFN can reduce the severity of CI-AKI by upregulating NRF2 expression. Thus, the present study aimed to establish models of CI-AKI in mice and HK-2 cells using cisplatin in order to elucidate the protective effect of SFN on CI-AKI and investigate the regulatory role of NRF2 expression in this condition.

Materials and methods

Establishment of a CI-AKI mouse model and SFN treatment. A total of 32 male C57BL/6 mice (age, 6-8 weeks; body weight, 20-25 g) was procured from the Experimental Animal Center of Nanjing Medical University (Nanjing, China) and maintained under specific pathogen-free conditions with *ad libitum* access to food and water (22±2˚C, Relative Humidity: 40-60%, Light/Dark Cycle: 12/12-h light/ dark cycle). Following a 7-day acclimation period, mice were randomly allocated into four experimental groups (n=6 per group), including control, SFN (10 mg/kg) (26), cisplatin (20 mg/kg, CAS No. 15663-27-1, Sigma-Aldrich) (27) and cisplatin + SFN groups. Starting from day 7 of the experiment, SFN was administered daily to mice in the relevant groups, whereas control and cisplatin-only groups received equivalent volumes of saline. After 7 days of pre-treatment with SFN or saline, mice in the cisplatin and cisplatin + SFN groups received a single intraperitoneal injection of cisplatin (20 mg/kg in saline). Euthanasia was performed 72 h after cisplatin administration via intraperitoneal injection of 5% sodium pentobarbital (150 mg/kg).

To confirm mortality following euthanasia, mice underwent checks for: i) Cardiac and respiratory arrest; ii) pain responses; and iii) pupillary responses to light stimuli. Blood samples were immediately collected via terminal cardiac puncture. A total of 0.8-1.0 ml of blood was extracted per mouse into serum-separating tubes. Serum was obtained by centrifugation of blood samples at 3,000 g for 15 min at 4˚C and samples were stored at -80˚C for subsequent analysis. During the study, the following humane endpoints were established and strictly observed: i) Severe lethargy or unresponsiveness to stimuli; ii) loss of >20% body weight; iii) inability to access food or water; and iv) signs of severe distress, for example labored breathing or hunched posture (28). No mice were euthanized prematurely due to reaching predetermined humane endpoints. All procedures and were approved by the Ethics Committee of Nanjing Medical University (approval no. IACUC 2024-0811).

Cell culture and treatment. The human proximal tubular epithelial cell line HK-2 was obtained from the American Type Culture Collection. Cells were maintained in DMEM/F-12 supplemented with 10% fetal bovine serum (FBS; both Gibco; Thermo Fisher Scientific, Inc.) and 1% penicillin-streptomycin solution comprising 100 U/ml penicillin and 100 μg/ml streptomycin under standard culture conditions (37˚C; 5% CO_2 humidified atmosphere). Upon achieving 70% confluence, cells were serum-starved by switching to FBS-free medium. Prior to experimental treatments, cells were pre-treated with one or both of 5 μM SFN and 1.9 μM ML385, an NRF2 inhibitor, dissolved in dimethyl sulfoxide for 4 h (37˚C). Following pre-treatment, cellular models were established by exposing HK-2 cells to 10 μg/ml cisplatin for 24 h (37˚C) (27). For the control group, cells were cultured in PBS-free medium without pre-treatment or cisplatin.

Blood biochemical analysis. Serum samples from mice in each treatment group were analyzed to quantify specific biomarkers, namely blood urea nitrogen (BUN; Jianglai Biotechnology Co., Ltd. (Cat. No. JL12567) with 50 μl of serum per well, serum creatinine (Scr) from Nanjing Jiancheng Bioengineering Institute (Cat. No. C011-2-1) with 20 μl of serum per well, MDA from Xitang Biotechnology Co., Ltd. (Cat. No. XT-MDA-001) with 10 μl serum per well, SOD from Abcam (Cat. No. ab65354) using 15 μl of serum per well and GSH from Kaiji Biotechnology Co., Ltd. (Cat. No. KGA7305) with 50 μl of serum per well. All biochemical analyses followed established protocols provided by the manufacturer's instructions.

ELISA. Serum and cell supernatant samples underwent centrifugation at 3,000 x g for 10 min at 4˚C. The levels of IL-1β, IL-6 and TNF-α were measured using ELISA kits according to the instructions provided by the manufacturer (IL-1β, Elabscience Biotechnology Co., Ltd., No. E-EL-M0059), (IL-6, Elabscience Biotechnology Co., Ltd., No. E-EL-M0044) and (TNF-α, all Elabscience Biotechnology Co., Ltd., No. E-EL-M0059, E-EL-M0049).

Hematoxylin and eosin (H&E) staining. Mouse renal tissues were fixed in 4% PFA at 4˚C for 24 h, then embedded in paraffin. After dewaxing, tissue sections (4 μm) were rehydrated using gradient ethanol. Sections were subsequently stained with hematoxylin for 10 min, rinsed with tap water for 2 sec and then stained with eosin for 5 min. After rinsing with tap water for 1 sec, the sections were dehydrated in gradient ethanol at 75, 95 and 100%, each for 5 sec, and subsequently air-dried. All procedures were performed at room temperature. Changes to mouse renal structure were observed under a light microscope in five randomly-selected visual fields.

Periodic acid-Schiff (PAS) staining. PAS staining was performed on 4 μm-thick paraffin-embedded mouse renal sections. The renal tissues were fixed in 4% paraformaldehyde at 4˚C overnight before embedding. After deparaffinization in xylene and hydration in a graded ethanol series, tissue sections were oxidized with 0.5% periodic acid for 10 min and subsequently stained with Schiff reagent for 30 min to detect polysaccharides and glycoproteins at room temperature. Nuclei were counterstained with Mayer's hematoxylin for 1 min and sections were subsequently differentiated in acid alcohol and blued in alkaline solution for 2 min at room temperature. Following dehydration through an ethanol-xylene series, sections were mounted with resin medium. Staining patterns in five randomly selected were visualized using bright-field light microscopy at x20 magnification.

TUNEL staining. Briefly, 5-μm paraffin-embedded renal tissue sections and cultured HK-2 cells grown on coverslips were fixed in 4% paraformaldehyde (PFA) for 1 h at room temperature. Samples were subsequently permeabilized using 0.1% Triton X-100 in 0.1% sodium citrate for 30 min on ice. After washing with PBS, samples were incubated with TUNEL reaction (One-Step TUNEL Apoptosis Assay kit, Green Fluorescence, Catalog No. KTA2010, Abbkine, Wuhan, China) mixture for 1 h at 37˚C in a humidified chamber. Nuclei were counterstained with 1 μg/ml DAPI for 5 min (22-25˚C). Slides were mounted with antifade mounting medium and images of five randomly selected fields of view were captured using a fluorescence microscope.

2',7'-dichlorodihydrofluorescein diacetate (DCFH-DA) analysis. ROS levels were quantified using the fluorescent probe DCFH-DA. For the HK-2 cell line, cells (1-5x10^5) were cultured to 70-80% confluence in 6-well plates, washed with PBS and subsequently incubated with 10 μM DCFH-DA in serum-free medium for 30 min at 37˚C in the dark. Cells were then washed twice with ice-cold PBS to remove extracellular dye. Finally, ROS levels in different treatment groups were analyzed by flow cytometry.

For mouse renal tissue samples, sections were equilibrated in PBS (pH 7.4) for 10 min at 37˚C and incubated with 10 μM DCFH-DA dissolved in serum-free DMEM (Gibco, No. 12634010) for 30 min in the dark at 37˚C. Excess probe was removed by gently washing the sections three times with PBS to minimize background fluorescence. Data were analyzed using FACSCelesta™ and FlowJo™ Software Version 10.8.1 from BD Biosciences.

Immunohistochemistry (IHC). Tissue sections (-80˚C) were thawed using PBS solution and subsequently dried using absorbent paper. Sections (5-10 μm) underwent fixation with

4% PFA for 20 min at room temperature. Following rinsing with PBS, sections were treated with 0.1% Triton X-100 for 5 min at room temperature. Endogenous peroxidase activity was blocked with 3% hydrogen peroxide in methanol for 15 min at room temperature. Sections were then blocked using a solution of 5% bovine serum albumin (BSA) (Sigma-Aldrich, No. A7906) for 1 h at room temperature and incubated with the primary antibodies (F4/80, Abcam, ab300421) 1:500, NRF2 (Abcam, ab313825) 1:100) overnight at 4˚C. Following three washes with PBS, sections were incubated with the secondary antibody (Goat Anti-Mouse IgG H&L (HRP) (Abcam, ab205719) 1:2,000) for 1 h at room temperature. Samples underwent DAPI (Vector Laboratories, No. SK-4100) staining for 5 min at room temperature to visualize nuclei and were sealed beneath a coverslip. Finally, images were captured with a light microscope.

Immunofluorescence staining. HK-2 cells ($5x10^4$ to $1x10^5$) in the logarithmic growth phase were lifted and centrifuged (1,000 x g for 5 min at room temperature), and the cell density was adjusted for inoculation in 12-well plates at 37˚C with 5% CO_2 overnight, with three replicate wells prepared for each group. Cells were fixed with 4% PFA for 30 min at room temperature, followed by permeabilization with 0.1% (v/v) Triton X-100 (Sigma-Aldrich, No. T8787) in PBS at room temperature for 10 min to disrupt the cell membrane. Following permeabilization, samples were blocked with 5% (w/v) BSA in PBS containing 0.1% Tween-20 at room temperature for 60 min. Then cells were incubated with primary antibodies (Nrf2 (Abcam, ab313825) 1:500) overnight. Samples were washed to remove excess primary antibodies 4˚C overnight and incubated with secondary antibodies (Goat Anti-Rabbit IgG H&L (HRP; Abcam, ab6721) 1:2,000) for 2 h at room temperature. Following this incubation, secondary antibodies were washed off and cells were incubated for 15 min with DAPI staining solution at room temperature. Samples were washed again and images of cells were captured using a fluorescence microscope.

Cell counting kit-8 (CCK-8) assay. To assess the viability of HK-2 cells, a CCK-8 assay was performed (Beyotime Biotechnology) in accordance with the manufacturer's instructions. HK-2 cells (5,000 cells) were seeded into 96-well plates, which were incubated for 48 h. Subsequently, 10 μl CCK-8 reagent was introduced into each well and the plates were incubated for a duration of 2 h. The absorbance of samples was then quantified at a wavelength of 450 nm using a microplate reader (SMR60047 Smart Microplate Reader, manufactured by USCNK Life Science Co. Ltd.). All incubation steps were performed at 37˚C with 5% CO_2.

Cell apoptosis. HK-2 cells were harvested following centrifugation at 300 x g for 5 min at 4˚C, washed twice with cold PBS and resuspended in 1X binding buffer at a density of $1x10^6$ cells/ml. Subsequently, 100 μl cell suspension was incubated with 5 μl annexin V-FITC and 5 μl propidium iodide in the dark for 15 min at room temperature. Samples were analyzed immediately using a BD FACSCanto™ II flow cytometer (BD Biosciences) and using FlowJo v10.8.1 (BD Biosciences, USA).

Reverse transcription-quantitative polymerase chain reaction (RT-qPCR) analysis. RT-qPCR was utilized to analyze the mRNA expression of NRF2. TRIzol (Thermo Fisher Scientific, Inc.) was used to extract RNA from HK-2 cells and cDNA was synthesized utilizing the PrimeScript™ RT Reagent Kit (Takara Bio Inc.), according to the manufacturer's instructions. qPCR was conducted using the SYBR-Green PCR Master Mix (Applied Biosystems; Thermo Fisher Scientific, Inc.) on a GeneAmp® PCR System 9700 (Applied Biosystems; Thermo Fisher Scientific, Inc.). The primer sequences used were as follows: NRF2, forward 5'-GCCACCGCCAGGACT ACAG-3', reverse 5'-GCAACAAGAGCAGCCACCTC-3'; and GAPDH, forward 5'-CCCTCGTCCCGTAGACAAAATG-3', reverse 5'-TGAGGTCAATGAAGGGGTCGT-3'. The thermocycling conditions for the qPCR reaction included an initial denaturation step at 95˚C for 30 sec, followed by 40 cycles of denaturation at 95˚C for 10 sec and annealing and extension at 60˚C for 10 sec. GAPDH served as the internal control, and the relative expression levels of NRF2 were assessed using the $2^{-\Delta\Delta Cq}$ analysis method (29).

Western blot analysis. Total protein was extracted from HK-2 cells and mouse renal tissues using RIPA buffer (Beyotime Biotechnology) in the presence of protease inhibitors. A BCA Protein Assay Kit (Beyotime Biotechnology) was used to determine the total protein content of the samples. Proteins (20-30 μg/lane) were separated using 10% SDS-PAGE and subsequently transferred via electrophoresis onto a polyvinylidene fluoride membrane. Membranes were blocked for 1 h with 5% skimmed milk powder in Tris-buffered saline + 20% Tween-20 (TBST) at room temperature. Membranes were incubated with primary antibodies (KIM-1 (Proteintech, 30948-1-AP) 1:500, NGAL (Proteintech, 31721-1-AP) 1:500, Bax (Proteintech, 50599-2-Ig) 1:500, Bcl-2 (all Proteintech, 68103-1-Ig) 1:500, Cleaved caspase-3 (Abcam, ab214430), Caspase-3 (Abcam, ab184787) 1:500, NRF2 (Abcam, ab313825) 1:500, GAPDH (all Abcam, ab181602; all 1:500) overnight at 4˚C. Membranes were washed with TBST solution and treated with HRP-conjugated goat anti-rabbit secondary antibodies for 1 h at room temperature. Protein bands were visualized utilizing an ECL reagent (Thermo Fisher Scientific, Inc.), and analyzed by ImageJ (Version 1.54, developed by the National Institutes of Health).

Statistical analysis. All experimental data are presented as the mean ± standard deviation of three independent experimental repeats. Data were analyzed using GraphPad Prism 7.0 (Dotmatics). Data were analyzed using unpaired t-test or one-way ANOVA followed by Tukey's post hoc test. $P<0.05$ was considered to indicate a statistically significant difference.

Results

SFN protects against CI-AKI in mice. To explore the role of SFN in the development and progression of CI-AKI, the present study established a mouse model of CI-AKI, and mice were separated into groups for treatment with or without SFN. As shown in Fig. 1A, the levels of Scr and BUN in the CI-AKI model group were significantly higher than the control group, whereas SFN treatment significantly attenuated the heightened

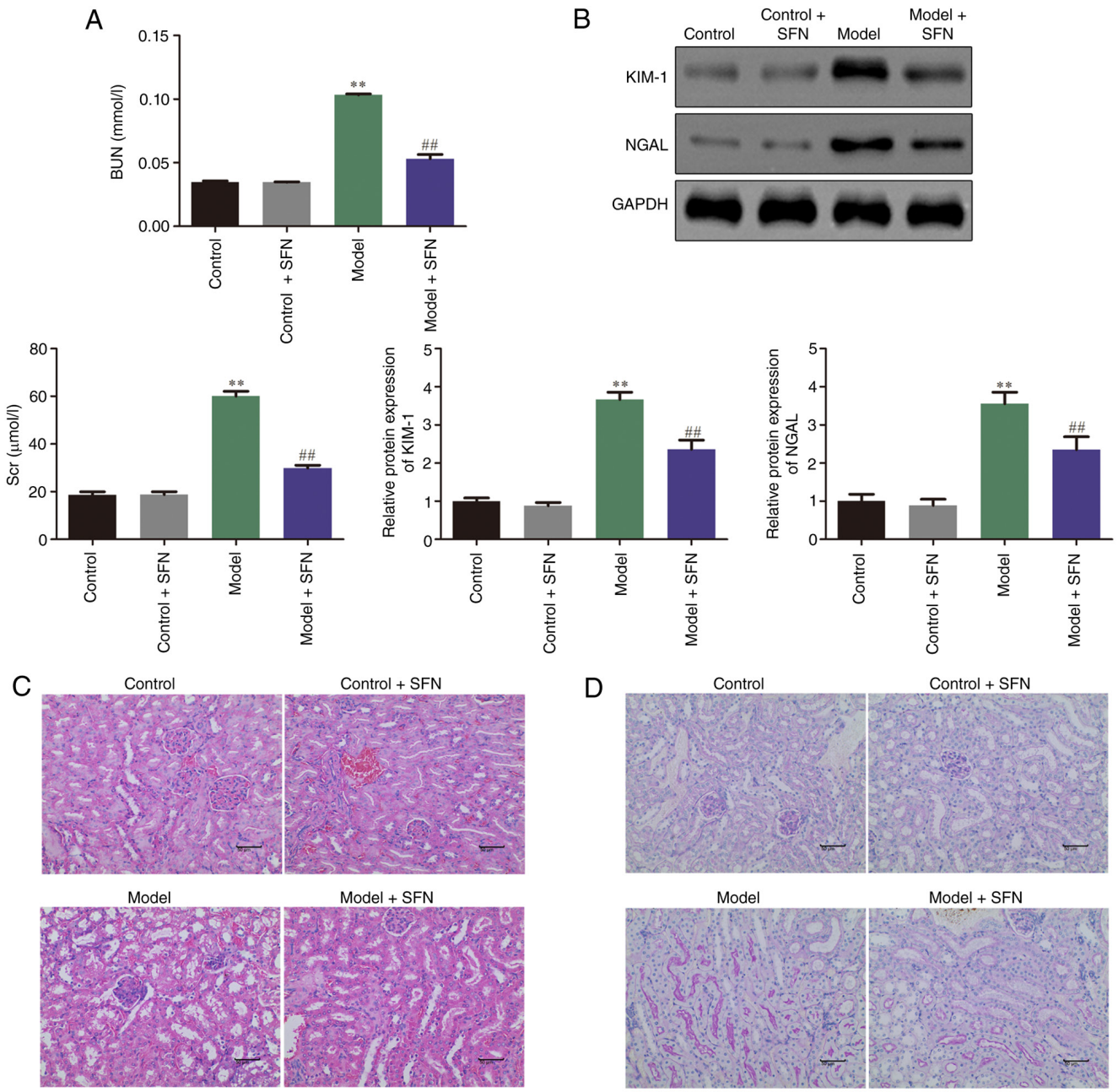

Figure 1. SFN protects against cisplatin-induced acute kidney injury in mice. (A) BUN and Scr levels in the serum of mice in control, control + SFN, model and model + SFN groups. (B) KIM-1 and NGAL levels in control and cisplatin-induced model mice treated with or without SFN. Representative images of (C) H&E and (D) PAS staining of mouse kidney tissue (x20 magnification). Data are shown as mean ± SD. **P<0.01 vs. control group; $^{\#\#}$P<0.01 vs. model group. SFN, sulforaphane; BUN, blood urea nitrogen; Scr, serum creatinine; KIM-1, kidney injury molecule-1; NGAL, neutrophil gelatinase-associated lipocalin; H&E, hematoxylin and eosin; PAS, periodic acid-Schiff.

levels of Scr and BUN. Mouse kidney markers were measured to determine the extent of pathological damage to the kidneys in different treatment groups. The protein expression of kidney injury molecule-1 (KIM-1) and neutrophil gelatinase-associated lipocalin (NGAL) was significantly increased in the model group compared with the control group, whereas SFN significantly reduced the expression of KIM-1 and NGAL in the model + SFN group compared with the model group (Fig. 1B). Furthermore, H&E and PAS staining were performed to investigate whether SFN improved the renal pathology of CI-AKI in model mice. As demonstrated in Fig. 1C and D, the results of both H&E and PAS staining indicated that epithelial cells in the control group exhibited intact morphology and were arranged neatly, whereas the renal pathological structure of cisplatin-treated model mice demonstrated notable damage, such as irregular morphology and detachment of renal tubular epithelial cells, marked dilation of renal tubules and vacuolar degeneration of renal tubules. Compared with the model group, kidney damage after prophylactic administration of SFN was markedly reduced. Furthermore, administration of SFN to control mice showed no effects on Scr and BUN, KIM-1 and NGAL and renal pathology (Fig. 1A-D) compared with the control group. These findings indicated that SFN ameliorated CI-AKI in mice.

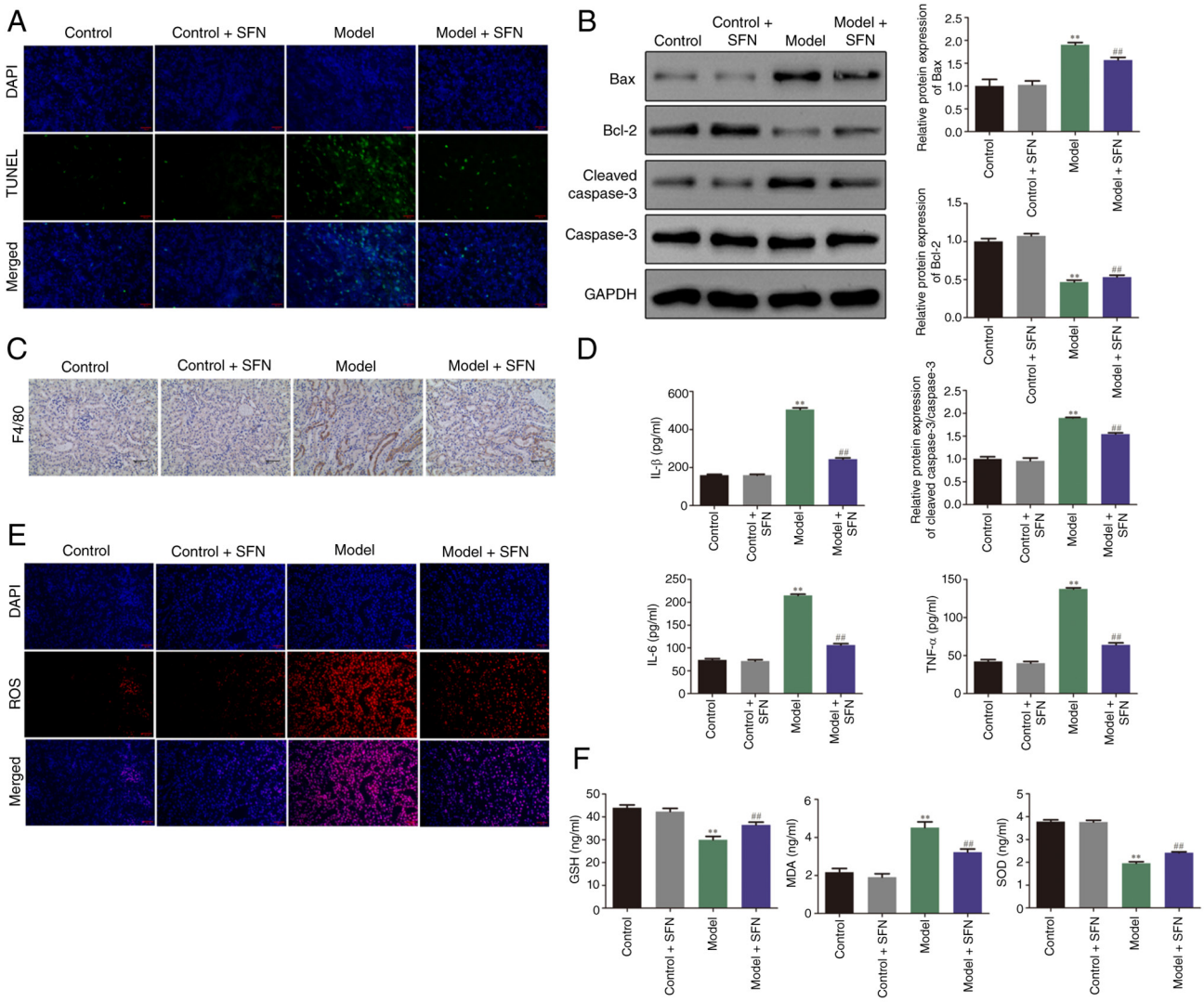

Figure 2. SFN inhibits cisplatin-induced apoptosis, inflammation and oxidative stress. (A) TUNEL staining was used to determine the number of apoptotic TUNEL-positive cells in the renal tubular lumen of mice in each treatment group. Magnification, x10 magnification). (B) Expression levels of the apoptosis-related proteins Bax, Bcl-2, cleaved caspase-3 and caspase-3 in mice were detected via western blotting. (C) Representative images of immunohistochemical analysis showing F4/80 expression in control and model mice treated with or without SFN (x20 magnification). (D) ELISA was performed to evaluate the expression of IL-1β, IL-6 and TNF-α in mice across treatment groups. (E) 2',7'-dichlorodihydrofluorescein diacetate staining was performed to evaluate the expression of ROS in mice in each treatment group (x10 magnification). (F) Biochemical analysis was used to evaluate the expression levels of MDA, SOD and GSH of mice in each group. **P<0.01 vs. control group; $^{\#\#}$P<0.01 vs. model group. SFN, sulforaphane; IL, interleukin; TNF-α, tumor necrosis factor-α; MDA, malondialdehyde; SOD, superoxide dismutase; GSH, glutathione; ROS, reactive oxygen species.

SFN inhibits cisplatin-induced apoptosis, inflammation and oxidative stress. Apoptosis, inflammation and oxidative stress serve important roles in the progression of CI-AKI (30). As shown in Fig. 2A, the number of TUNEL-positive cells in the renal tubular lumen of cisplatin-treated model mice was notably increased compared with the control group, and treatment with SFN markedly reduced the apoptosis of renal tubular cells in model mice. Furthermore, the levels of apoptosis-related proteins, namely Bax, Bcl-2, cleaved caspase-3 and caspase-3, were detected via western blot assay. Compared with the control group, the expression of the pro-apoptotic protein Bax and the ratio of cleaved caspase-3/caspase-3 in the kidneys of mice treated with cisplatin were significantly increased, whereas the expression level of the anti-apoptotic protein Bcl-2 significantly decreased. SFN treatment in model mice significantly alleviated these changes (Fig. 2B). Furthermore, the levels of inflammatory indicators, such as F4/80, IL-1β, IL-6 and TNF-α, were measured via IHC and ELISA. As shown in the representative immunohistochemistry images in Fig. 2C, F4/80 levels were markedly increased in the model group compared with the control group. However, treatment of model mice with SFN resulted in a notable decrease in F4/80 levels compared with untreated model mice. Similarly, IL-1β, IL-6 and TNF-α were significantly upregulated in the model compared with the control group; however, these levels were significantly reduced in the model + SFN group compared with the model group (Fig. 2D). Furthermore, DCFH-DA staining was used to visualize ROS levels in each treatment group. Staining results revealed that ROS levels were markedly increased in the model group compared with the control group. However, ROS levels were notably attenuated in the model + SFN group compared with the model group (Fig. 2E). Similarly, biochemical analysis was utilized to evaluate the expression levels of MDA, SOD and GSH. As demonstrated in

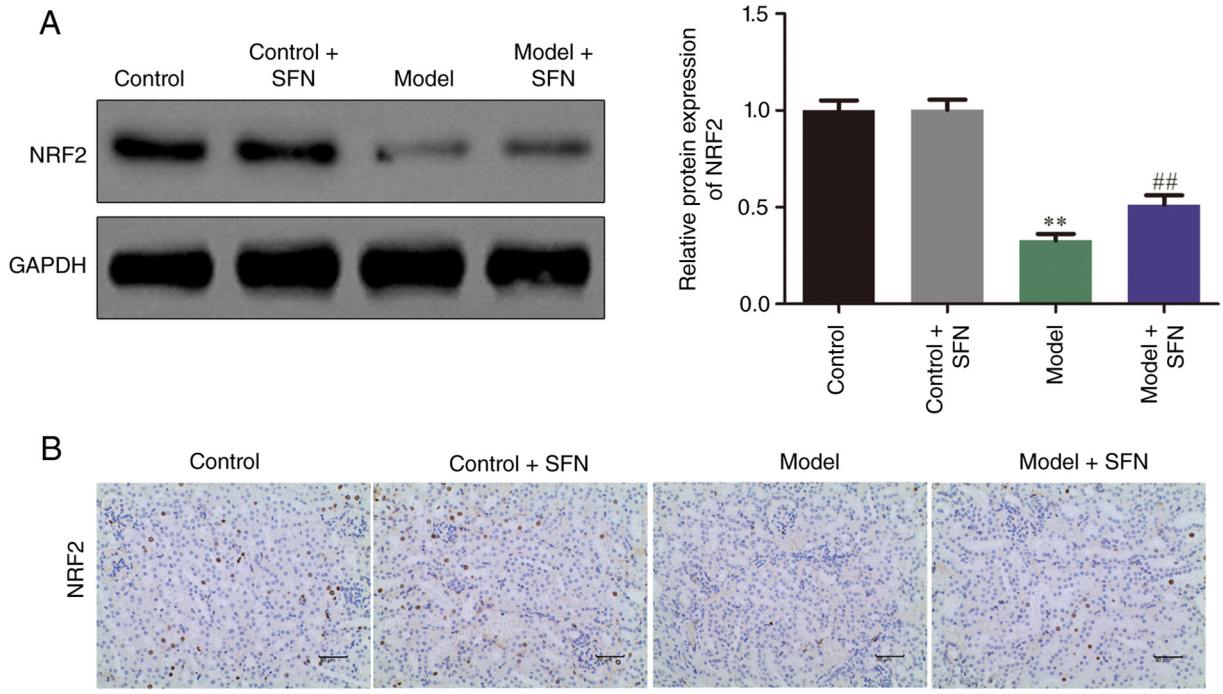

Figure 3. SFN activates the NRF2 signaling pathway. (A) NRF2 expression was detected in each group via western blotting and semi-quantified. (B) Representative images of immunohistochemical analysis in each group (x20 magnification). **P<0.01 vs. control; $^{\#\#}$P<0.01 vs. model group. SNF, sulforaphane; NRF2, nuclear factor erythroid-2-related factor 2.

Fig. 2F, compared with the control group, MDA in the model group was significantly upregulated, and the levels of SOD and GSH were significantly decreased. However, compared with the model group, SFN treatment significantly mitigated MDA levels and partially yet significantly restored SOD and GSH levels. These findings indicated that SFN inhibited cisplatin-induced apoptosis, inflammation and oxidative stress.

SFN activates the NRF2 signaling pathway. The NRF2 signaling pathway, as one of the major signal transduction pathways in CI-AKI, plays an important role in the progression and development of CI-AKI (31). IHC and western blotting were performed to determine the effects of SFN on the expression of NRF2. As shown in Fig. 3, SFN upregulated the expression of NRF2 signaling pathway in CI-AKI mice compared with untreated model mice. These findings indicated that SFN ameliorated CI-AKI in mice by upregulating NRF2.

SFN protects HK-2 cells against cisplatin-induced apoptosis, inflammation and oxidative stress in vitro partially by regulating the NRF2 signaling pathway. To further investigate the protective effect and mechanisms of SFN in HK-2 cells *in vitro*, the present study evaluated changes in cell apoptosis, inflammation and oxidative stress. CCK-8 assay indicated that, compared with the control group, cisplatin significantly inhibited the viability of HK-2 cells, whereas treatment of cisplatin-induced cells with SFN mitigated this effect (Fig. 4A). Flow cytometry, DCFH-DA staining and ELISA demonstrated that cisplatin significantly promoted apoptosis, inflammation and oxidative stress in HK-2 cells relative to the control group. Notably, treatment of model cells with SFN significantly mitigated cisplatin-induced apoptosis, inflammation and oxidative stress (Fig. 4B-D). Furthermore, the present study performed RT-qPCR, western blotting and immunofluorescence staining to assess the expression of NRF2. As indicated in Fig. 4E-G, treatment with SFN significantly upregulated NRF2 in cisplatin-induced HK-2 cells compared with the model group. Furthermore, co-treatment with the NRF2 inhibitor ML385 partially yet significantly mitigated the effects of SFN on the viability, apoptosis, inflammation and oxidative stress of HK-2 model cells induced with cisplatin (Fig. 4A-D). These findings indicated that SFN protected HK-2 cells against cisplatin-induced apoptosis, inflammation and oxidative stress *in vitro* via regulation of the NRF2 signaling pathway.

Discussion

Cisplatin is one of the most widely used anticancer drugs globally and is used in ~50% of chemotherapy regimens (32). The kidney is the predominant organ responsible for cisplatin metabolism, and the concentration of cisplatin in the proximal renal tubules during chemotherapy is ~5-fold that of the blood, therefore cisplatin is prone to accumulate in the kidney (5). Upon accumulation, cisplatin generates a large amount of ROS in the kidneys, which triggers oxidative stress and inflammatory cascade reactions, ultimately leading to kidney cell apoptosis or necrosis. This causes notable kidney damage and limits the clinical application of cisplatin (33). Therefore, preventing or mitigating CI-AKI is important for improving the clinical application of cisplatin.

SFN is an isothiocyanate, which are products of the myrosinase-mediated hydrolysis of glucosinolates found in cruciferous vegetables, such as broccoli (34). It has been reported that SFN exhibits anti-inflammatory, antioxidant, antitumor and immunosuppressive activities and plays a therapeutic role in diabetes nephropathy and psoriasis (35).

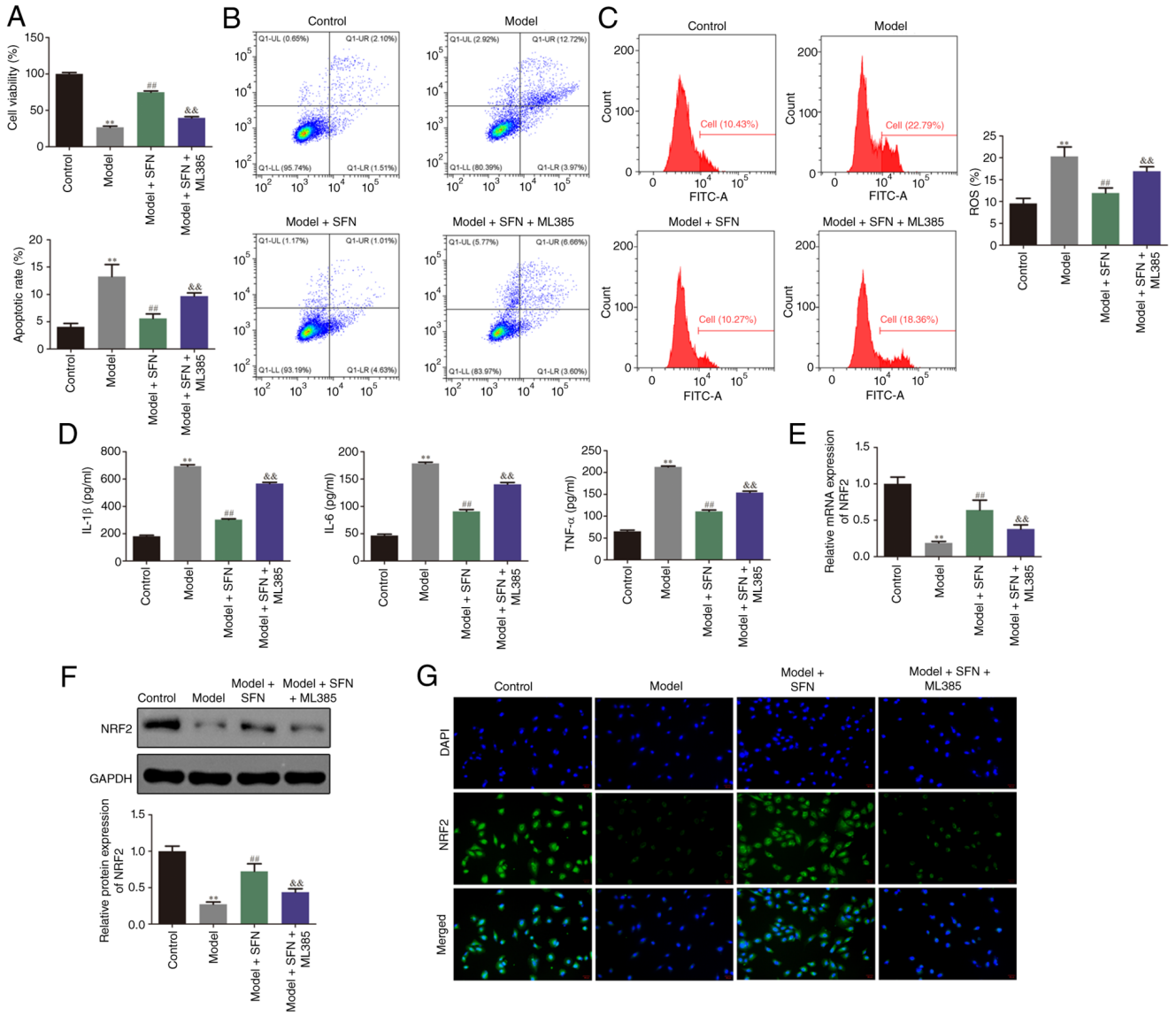

Figure 4. SFN protects HK-2 cells against cisplatin-induced apoptosis, inflammation and oxidative stress *in vitro* by regulating the NRF2 signaling pathway. (A) Viability of HK-2 cells in different treatment groups was evaluated by Cell Counting Kit-8 assay. (B) Flow cytometry was performed to evaluate the apoptosis of HK-2 cells in different groups. (C) 2',7'-dichlorodihydrofluorescein diacetate analysis was performed to evaluate ROS levels in HK-2 cells. (D) ELISA was performed to evaluate the levels of inflammatory markers IL-6, IL-1β and TNF-α in HK-2 cells across treatment groups. (E) Reverse transcription-quantitative PCR, (F) western blotting and (G) immunofluorescence staining were performed to evaluate the expression of NRF2 in HK-2 cells across different groups (x10 magnification). **P<0.01 vs. control group; $^{\#\#}$P<0.01 vs. model group; $^{\&\&}$P<0.01 vs. SFN group. SFN, sulforaphane; ROS, reactive oxygen species; IL, interleukin; TNF-α, tumor necrosis factor-α.

A previous study demonstrated that SFN prevents cell death and inflammation in diabetic nephropathy, highlighting its broad renoprotective potential (36). However, to the best of our knowledge, no in-depth research has been performed to elucidate whether SFN exerts protective effects against CI-AKI. To the best of our knowledge, the present study demonstrated for the first time that SFN exhibited a protective effect in CI-AKI. The present study explored the protective mechanisms of SFN from three aspects, namely oxidative stress, inflammation and cell apoptosis, with a specific focus on elucidating the role of the NRF2 signaling pathway in mediating these effects.

Serum levels of BUN and Scr can reflect glomerular filtration function. When renal function is impaired, the concentrations of these biomarkers in the blood are notably increased due to reduced excretion from the kidneys. Histopathological examination can also reflect the survival status of kidney cells (6). The results of animal experiments in the present study showed that the concentrations of BUN and Scr in the serum of mice treated with cisplatin alone were increased compared with controls. H&E and PAS staining of renal tissues showed that cisplatin induced pathological changes. The levels of renal function indicators in model mice treated with SFN were significantly reduced compared with untreated model mice and demonstrated notable improvements to the pathological damage of kidney tissue, indicating that SFN had a protective effect on CI-AKI.

ROS, including peroxides, superoxide and hydroxyl radicals, are important factors in cisplatin-induced oxidative

stress, inflammatory responses and cell apoptosis. MDA is an important indicator for measuring lipid peroxidation and oxidative damage, whereas SOD can inhibit lipid peroxidation by clearing superoxide anion radicals in the body (37). GSH is one of the most important non-enzymatic antioxidants, demonstrating multiple functions, including the clearance of free radicals, detoxification and the maintenance cell immunity (38). The excessive production of ROS leads to the excessive consumption of antioxidants, including SOD and GSH, resulting in lipid peroxidation and the generation of excess MDA, resulting in cell or tissue damage (39). Therefore, the combined detection of ROS, MDA, SOD and GSH was used to determine the degree of lipid peroxidation damage in mice.

In addition, ROS promote the production of pro-inflammatory cytokines, for example TNF-α, IL-6 and IL-1β, inducing a cascade of inflammatory reactions and exacerbating kidney damage. As ROS levels increase, lipids, proteins and nucleic acids in renal cells become damaged, leading to cell apoptosis or necrosis (40). The *in vivo* experiments of the present study demonstrated that the levels of ROS, MDA, TNF-α, IL-6 and IL-1β were significantly increased in cisplatin-induced mice, whereas the levels of SOD and GSH were significantly reduced. In addition, cisplatin notably induced the apoptosis of renal tubular cells. Intervention with SFN was shown to significantly attenuate the aforementioned pathological changes in model mice.

In order to further investigate the effects of SFN on cisplatin-induced oxidative stress, inflammatory responses and cell apoptosis, the present study constructed an *in vitro* model of kidney injury using HK-2 cells. Flow cytometry was used to detect ROS levels in HK-2 cells, and the present study found that following cisplatin treatment, ROS levels in HK-2 cells were significantly increased. However, following intervention with SFN, ROS levels were significantly decreased, indicating that SFN alleviated oxidative stress caused by cisplatin. Furthermore, ELISA was used to detect changes in the levels of inflammatory factors, namely TNF-α, IL-6 and IL-1β. After cisplatin treatment for model establishment, TNF-α, IL-6 and IL-1β were significantly upregulated, whereas concurrent SFN intervention was significantly attenuate these heightened TNF-α, IL-6 and IL-1β levels, indicating that SFN alleviated inflammatory responses caused by cisplatin. Additionally, the present study evaluated the effects of SFN on the apoptosis of HK-2 cells and found that the number of apoptotic cells significantly increased following cisplatin treatment. Notably, the number of apoptotic cells was significantly reduced following SFN intervention of the model group, suggesting that SFN inhibited cisplatin-induced cell apoptosis. The aforementioned *in vitro* experimental results were consistent with the results of *in vivo* experiments, supporting the implication that the protective effects of SFN on CI-AKI were achieved by inhibiting oxidative stress, the inflammatory response and cell apoptosis.

NRF2 is a transcription factor that plays a protective role in oxidative damage (41). Activation of NRF2 is closely related to a decrease in ROS levels and an increase in antioxidant enzyme activity, and that NRF2 plays an important regulatory role in inhibiting oxidative stress and inflammatory responses to protect renal function (42). Under normal conditions, NRF2 binds to Kelch-like ECH-associated protein 1 (Keap1) in the cytoplasm. However, under conditions of oxidative stress, NRF2 dissociates from Keap1 and enters the nucleus, activating downstream antioxidant proteins, such as heme oxygenase-1 and NAD(P)H quinone dehydrogenase 1. This helps to maintain the dynamic balance of intracellular redox reactions, thereby protecting the body from damage caused by oxidative stress (43). Concurrently, activation of NRF2 can also inhibit the production of pro-inflammatory cytokines and alleviate the inflammatory response (44). In addition, NRF2 inhibits the activation of apoptotic pathways by suppressing oxidative stress. Under conditions of oxidative stress, increases in ROS levels disrupt the dynamic balance of mitochondrial integrity and enhance the activity of the apoptotic pathway by activating various signaling pathways, thereby inducing cell apoptosis (45).

In the present study, SFN intervention significantly upregulated NRF2, indicating that SFN may have alleviated cisplatin-induced oxidative stress, inflammatory responses and apoptosis by activating the NRF2 signaling pathway. To further support the direct regulatory role of the NRF2 signaling pathway in alleviating CI-AKI, the present study treated HK-2 cells with the NRF2 inhibitor ML385 to observe whether the regulatory effect of SFN on CI-AKI pathology was reversed. The results demonstrated that ML385 partially reversed the protective effects of SFN on oxidative stress, inflammatory responses and apoptosis in model HK-2 cells, suggesting that the renoprotective effect of SFN was partially regulated by activation of the NRF2 signaling pathway.

Although the present study was, to the best of our knowledge, the first study to demonstrate that SFN partially alleviated CI-AKI via activation of the NRF2 signaling pathway and provide evidence supporting its preventive administration, the present study exhibited several key limitations. In terms of experimental design, both animal and cell models employed a strict pre-treatment regimen involving a single dose of cisplatin and SFN, preventing a sufficient dose-response relationship analysis. Furthermore, the present study primarily evaluated the preventive potential of SFN and failed to simulate more common clinical intervention scenarios, such as post-injury or concurrent drug administration, which limited the elucidation of an effective and safe therapeutic window and the evaluation of SFN intervention efficacy in broader clinical application scenarios. In terms of mechanism verification, although the inhibitor ML385 experiment provided functional evidence of the involvement of the NRF2 pathway, the present study could not rule out the possibility that SFN may have employed other protective pathways that were not dependent on NRF2. Furthermore, the *in vitro* findings of the present study were based solely on the HK-2 cell line; future studies should include other relevant renal cell types to confirm the generalizability of the protective mechanisms. Therefore, future research should: i) Systematically optimize SFN dosages; ii) evaluate the efficacy of different SFN administration timings, such as the effect of post-injury treatment on CI-AKI; and iii) employ more in-depth molecular tools to verify the core role of NRF2 in the SFN-mediated alleviation of CI-AKI and explore parallel mechanisms

of SFN-mediated renoprotection in order to promote its clinical translation.

In summary, SFN exerted a protective effect on CI-AKI and demonstrated potential as an adjuvant drug for cisplatin treatment. The mechanisms underlying SFN-mediated protective effects may have been related to activation of the NRF2 signaling pathway, thereby mediating the inhibition of oxidative stress, the inflammatory response and cell apoptosis.

Acknowledgements

Not applicable.

Funding

The present study was supported by the Science and Technology Development Fund of Nanjing Medical University (grant nos. NMUB20220164 and NMUB20220057) and the Youth Fund of Nanjing Jiangning Hospital (grant no. JNYYZXKY202210).

Availability of data and materials

The data generated in the present study may be requested from the corresponding author.

Authors' contributions

ZW, MeL, HX, WL and JQ conceived and designed the study. LX, MiL and LS performed the experiments and analyzed data. HX and WL analyzed and interpreted data and drafted the original manuscript. ZW, MeL and JQ critically revised the manuscript. ZW and JQ confirmed the authenticity of the raw data generated during the study. All authors have read and approved the final version of the manuscript.

Ethics approval and consent to participate

The present study was reviewed and approved by the Ethics Committee of Nanjing Medical University (approval no. IACUC 2024-0811).

Patient consent for publication

Not applicable.

Competing interests

The authors declare that they have no competing interests.

References

1. Wei J and Zhu L: The role of glutathione peroxidase 4 in the progression, drug resistance, and targeted therapy of non-small cell lung cancer. Oncol Res 33: 863-872, 2025.
2. Sung HY, Han J, Ju W, Kang JL, Park AK and Ahn JH: MBNL2 enhances cisplatin resistance by regulating apoptosis in ovarian cancer cells. BMB Rep 58: 224-231, 2025.
3. Teixeira AR, Mata D, Ferreira H, Paiva A, Pelayo MJ, Rafael C, Maurício J, Calisto R and Cassiano Neves M: Short hydration regimen in cisplatin-based chemotherapy and its impact on nephrotoxicity: A unicentric prospective study. Cureus 17: e79774, 2025.
4. Sugino Y, Nishikawa T, Inaba S, Owa S, Kato M, Higashi S, Sasaki T, Masui S, Nishikawa K, Nakamura A, *et al*: Cisplatin-induced therapy-related myelodysplastic syndrome during avelumab maintenance therapy for metastatic urothelial carcinoma. Int Cancer Conf J 14: 73-78, 2025.
5. Tao S, Qi Y, Gao J, Yuan H, Wang R, Shen X, Wei G and Peng Z: Ameliorative effect of sipunculus nudus hydrolysate on cisplatin-induced nephrotoxicity by mitigating oxidative stress, inflammation and apoptosis. Mar Drugs 23: 100, 2025.
6. Park I, Kim S, Um YW, Kim HE, Lee JH, Kim S, Kim P and Jo YH: Intravital imaging of peritubular microcirculation impairment in cisplatin-induced acute kidney injury. JCI Insight 10: e178689, 2025.
7. Chen C, Wang W, Poklis JL, Li PL, Lichtman AH, Gewirtz DA and Li N: Mitigation of cisplatin-induced acute kidney injury through oral administration of fatty acid amide hydrolase inhibitor PF-04457845. J Pharmacol Exp Ther 392: 100032, 2025.
8. Bui AP, Pham TTM, Kim M, Park JH, Kim JI, Seo JH, Jung J, Kim JY and Ha E: GLDC alleviates cisplatin-induced apoptosis, cellular senescence, and production of reactive oxygen species via regulating UCP1 in the kidney. Life Sci 368: 123502, 2025.
9. Tian Z, Wu Y, Yi B, Li L, Liu Y, Zhang H and Li A: ESCRT III-mediated lysosomal repair improve renal tubular cell injury in cisplatin-induced AKI. Autophagy 21: 1927-1944, 2025.
10. Gu R, Shen J, Zhang J, Mao J and Ye Q: Revolutionizing autoimmune kidney disease treatment with chimeric antigen receptor-T cell therapy. Research (Wash D C) 8: 0712, 2025.
11. Oh CJ, Choi W, Lee HY, Lee IK, Kim MJ and Jeon JH: Sodium phenylbutyrate attenuates cisplatin-induced acute kidney injury through inhibition of pyruvate dehydrogenase kinase 4. Biomedicines 12: 2815, 2024.
12. Yang XP, Wang YJ, Xu YS, Peng S and Yuan HF: Bergamottin pretreatment attenuates cisplatin-induced acute kidney injury in mice by inhibiting BACE-1-mediated ferroptosis. Ren Fail 48: 2641847, 2026.
13. Airik M, Clayton K, Wipf P and Airik R: JP4-039 mitigates cisplatin-induced acute kidney injury by inhibiting oxidative stress and blocking apoptosis and ferroptosis in mice. Antioxidants (Basel) 13: 1534, 2024.
14. Zhang H, Deng Z, Wang Y, Zheng X, Zhou L, Yan S, Wang Y, Dai Y, Kanwar YS, Chen F and Deng F: CHIP drives proteasomal degradation of NUR77 to alleviate oxidative stress and intrinsic apoptosis in cisplatin-induced nephropathy. Commun Biol 7: 1403, 2024.
15. Yin H, Yan Q, Li Y and Tang H: Dihydromyricetin nanoparticles alleviate lipopolysaccharide-induced acute kidney injury by decreasing inflammation and cell apoptosis via the TLR4/NF-κB pathway. J Funct Biomater 15: 249, 2024.
16. Ji Y, Zhao Z, Yang Y, Wang X, Qiao R, Yu X, Gong X, Feng Z and Hong Q: Mechanisms underlying the impact of interleukin family on acute kidney injury: Pathogenesis, progression, and therapy. Research (Wash D C) 8: 0738, 2025.
17. Zhang Y, Hu J, Zhang Y and Ci X: Amentoflavone protects against cisplatin-induced acute kidney injury by modulating Nrf2-mediated oxidative stress and ferroptosis and partially by activating Nrf2-dependent PANoptosis. Front pharmacol 16: 1508047, 2025.
18. Ramadan SA, Kamel EM, Ewais MA, Khowailed AA, Hassanein EHM and Mahmoud AM: Flavonoids of Haloxylon salicornicum (Rimth) prevent cisplatin-induced acute kidney injury by modulating oxidative stress, inflammation, Nrf2, and SIRT1. Environ Sci Pollut Res Int 30: 49197-49214, 2023.
19. Liu J, Wang Y, Qiao P, Ying Y, Lin S, Lu F, Gao C, Li M, Yang B and Zhou H: Mechanisms of cisplatin-induced acute kidney injury: The role of NRF2 in mitochondrial dysfunction and metabolic reprogramming. Antioxidants (Basel) 14: 775, 2025.
20. Adtani PN, Al-Bayati SAAF and Elsayed WS: Sulforaphane from brassica oleracea induces apoptosis in oral squamous carcinoma cells via p53 activation and mitochondrial membrane potential dysfunction. Pharmaceuticals (Basel) 18: 393, 2025.
21. Song F, Verheust Y, Sampers I and Raes K: The stability of isothiocyanates in broccoli extract: Oxidation from erucin to sulforaphane was discovered. Food Chem 480: 143872, 2025.
22. Lv D, Chu L, Du Y, Li C, Bao N, Su Y, Wang G, Zheng Y and Yu Y: Sulforaphane alleviates membranous nephropathy by inhibiting oxidative stress-associated podocyte pyroptosis. Iran J Basic Med Sci 28: 237-244, 2025.
23. Josa E, Barril G and Ruperto M: Potential effects of bioactive compounds of plant-based foods and medicinal plants in chronic kidney disease and dialysis: A systematic review. Nutrients 16: 4321, 2024.

24. Zaghlool SS, Abdelaal N, El-Shoura EAM, Mahmoud NI and Ahmed YM: Restoring glomerular filtration rate by sulforaphane modulates ERK1/2/JNK/p38MAPK, IRF3/iNOS, Nrf2/HO-1 signaling pathways against folic acid-induced acute renal injury in rats. Int Immunopharmacol 123: 110777, 2023.
25. Li Z, Guo H, Li J, Ma T, Zhou S, Zhang Z, Miao L and Cai L: Sulforaphane prevents type 2 diabetes-induced nephropathy via AMPK-mediated activation of lipid metabolic pathways and Nrf2 antioxidative function. Clin Sci (Lond) 134: 2469-2487, 2020.
26. Pańczyszyn-Trzewik P, Stachowicz K, Misztak P, Nowak G and Sowa-Kućma M: Repeated sulforaphane treatment reverses depressive-like behavior and exerts antioxidant effects in the olfactory bulbectomy model in mice. Pharmaceuticals (Basel) 17: 762, 2024.
27. Xu N, Mu R, Deng S, Han Y, Shi Y, Fu X, Li H and Yao Q: Reserpine alleviates cisplatin-induced acute kidney injury via anti-ferroptosis and cGAS/STING pathway. Ren Fai 46: 2406395, 2024.
28. Cai F, Li D, Zhou K, Zhang W and Yang Y: Tiliroside attenuates acute kidney injury by inhibiting ferroptosis through the disruption of NRF2-KEAP1 interaction. Phytomedicine 126: 155407, 2024.
29. Livak KJ and Schmittgen TD: Analysis of relative gene expression data using real-time quantitative PCR and the 2(-Delta Delta C(T)) method. Methods 25: 402-408, 2001.
30. Zheng D, Ruan X, Wu Q, Qiu Y and Ruan S: Yishen Jiangzhuo decoction attenuates cisplatin-induced acute kidney injury by inhibiting inflammation, oxidative stress and apoptosis through the TNF signal pathway. Exp Ther Med 28: 331, 2024.
31. Zhao L, Yue Z, Wang G, Qin J, Ma H, Tang D and Yin G: Smilax glabra roxb. alleviates cisplatin-induced acute kidney injury in mice by activating the Nrf2/HO-1 signalling pathway. Phytomedicine 139: 156550, 2025.
32. Pan L, Zhang D, Shao Q, Cheng M, Liao Z, Yu L, Wang Y, Jia P and Zhang J: Panax notoginseng improves the sensitivity of non-small cell lung cancer to cisplatin by inhibiting Akt signaling. Cancer Biomark 42: 18758592241303377, 2025.
33. Abd-Eldayem AM, Ali MF and Ahmed EA: Nebivolol rescued the liver and kidney from the coadministration of rivaroxaban and cisplatin by targeting inflammation, oxidative stress, and apoptosis in rats. Int Immunopharmacol 153: 114486, 2025.
34. Liu Y and Zhang M: Synergistic anticancer effects of silibinin and sulforaphane: Targeting gastric cancer via PI3K/AKT and ERK1/2 MAPK pathway inhibition and molecular docking insights. J Biochem Mol Toxicol 39: e70237, 2025.
35. Zhao L, Li J, Dang Y, Fisher D, Hien NTT, Musabaev E, Pronyuk K and Zhao L: Protective role of sulforaphane in lipid metabolism-related diseases. Mol Biol Rep 52: 241, 2025.
36. Guerrero-Beltrán CE, Mukhopadhyay P, Horváth B, Rajesh M, Tapia E, García-Torres I, Pedraza-Chaverri J and Pacher P: Sulforaphane, a natural constituent of broccoli, prevents cell death and inflammation in nephropathy. J Nutr Biochem 23: 494-500, 2012.
37. Wu T, Ma W, Lu W, Huangshen Z, Chen S, Yang Q, Li C, Li Z, Li N, Feng X, *et al*: Vaccarin alleviates cisplatin-induced acute kidney injury via decreasing NOX4-derived ROS. Heliyon 9: e21231, 2023.
38. Ren Y, Wu F, Huo L, Wang X, Zhang Y, Fan M, Tan M, Zhao J, Cheng J, Zhao Z and Bao J: Switchable ROS generator and scavenger to prevent the cisplatin induced acute kidney injury and improve efficacy via synergistic chemodynamic/immune therapy. Mater Today Bio 29: 101328, 2024.
39. Li P, Li D, Lu Y, Pan S, Cheng F, Li S, Zhang X, Huo J, Liu D and Liu Z: GSTT1/GSTM1 deficiency aggravated cisplatin-induced acute kidney injury via ROS-triggered ferroptosis. Front Immunol 15: 1457230, 2024.
40. Qi J, Luo Q, Zhang Q, Wu M, Zhang L, Qin L, Xue Q and Nie X: Yi-Shen-Xie-Zhuo formula alleviates cisplatin-induced AKI by regulating inflammation and apoptosis via the cGAS/STING pathway. J Ethnopharmacol 309: 116327, 2023.
41. Hu J, Zhang Y, Zhang Y, Shi N, Miu Y, Huang J, Miao M and Ci X: Bergenin inhibits ferritinophagy and ferroptosis in cisplatin-induced acute kidney injury by activating the p-GSK3β/Nrf2/PPARγ pathway. Int Immunopharmacol 147: 114004, 2025.
42. Qi H, Shi H, Yan M, Zhao L, Yin Y, Tan X, Qi H, Li H, Weng K, Tang Y and Dai Y: Ammonium tetrathiomolybdate relieves oxidative stress in cisplatin-induced acute kidney injury via NRF2 signaling pathway. Cell Death Discov 9: 259, 2023.
43. Wang S, Zheng Y, Jin S, Fu Y and Liu Y: Dioscin protects against cisplatin-induced acute kidney injury by reducing ferroptosis and apoptosis through activating Nrf2/HO-1 signaling. Antioxidants (Basel) 11: 2443, 2022.
44. Sami DH, Soliman AS, Khowailed AA, Hassanein EHM, Kamel EM and Mahmoud AM: 7-Hydroxycoumarin modulates Nrf2/HO-1 and microRNA-34a/SIRT1 signaling and prevents cisplatin-induced oxidative stress, inflammation, and kidney injury in rats. Life Sci 310: 121104, 2022.
45. Hu J, Gu W, Ma N, Fan X and Ci X: Leonurine alleviates ferroptosis in cisplatin-induced acute kidney injury by activating the Nrf2 signalling pathway. Br J Pharmacol 179: 3991-4009, 2022.